Electronic Supplementary Material (ESI) for RSC Advances.
This journal is © The Royal Society of Chemistry 2017

A multianalyte fluorescent carbon dots sensing system constructed based on specific recognition of Fe(III) ions

Electronic supplementary information for

Pei Song,[a] Lisha Zhang,[a] Hao Long,[a] Meng Meng,[a] Ting Liu,[b] Yongmei Yin,*[a] Rimo Xi,*[a]

[a] State Key Laboratory of Medicinal Chemical Biology, College of Pharmacy and Tianjin Key Laboratory of Molecular Drug Research, Nankai University, Tianjin 300353, China

[b] Tianjin Medical University Eye Hospital, Tianjin 300384, China

***Corresponding Author:**

Tel: +86-(22)-23506290; Fax: +86-(22)-23507760;

Yongmei Yin: E-mail: yinyongmei@nankai.edu.cn

Rimo Xi: E-mail: xirimo@nankai.edu.cn

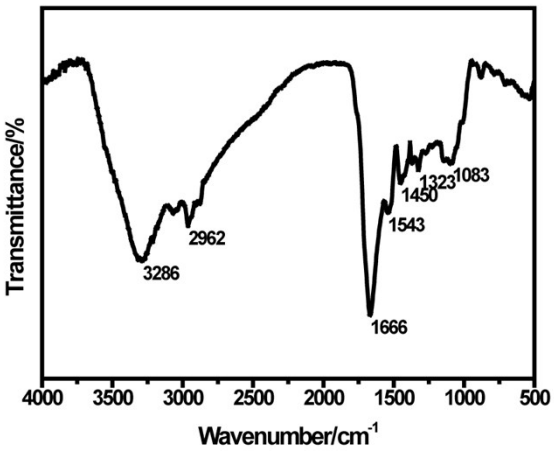

Fig. S1 FTIR spectra of the as-prepared CDs.

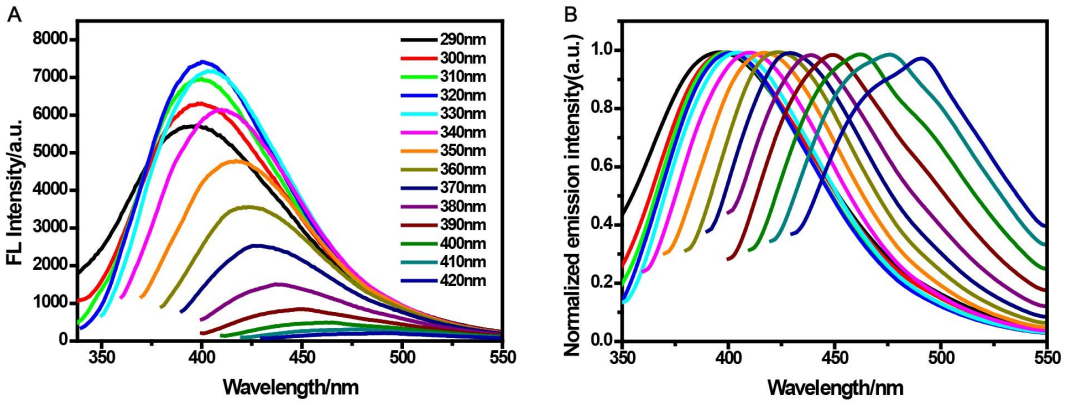

Fig. S2 (A) Fluorescent emission spectra of the CDs at different excitation wavelengths ranging from 290 nm to 420 nm with increments of 10 nm. (B) Normalized fluorescent emission spectra of CDs (Excitation wavelengths ranged from 290 nm to 420 nm).

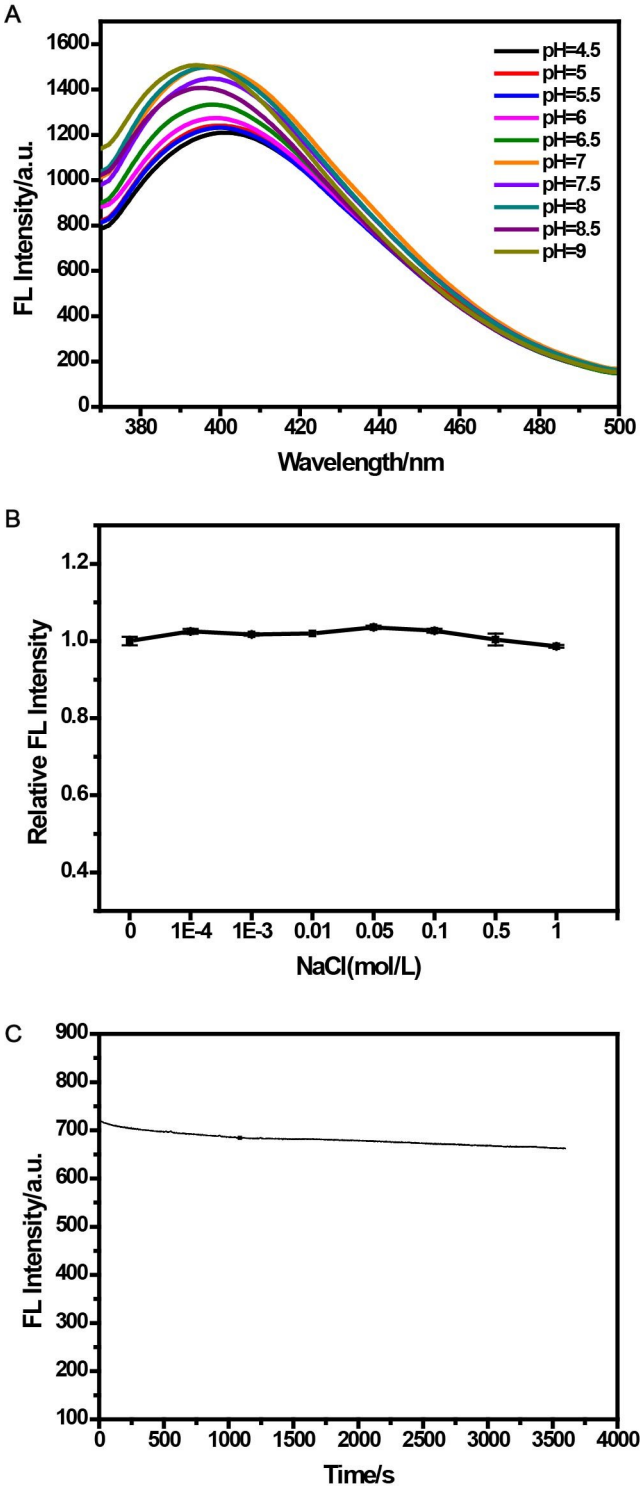

Fig. S3 Fluorescence intensity variation of CDs at different pH values (A), different ionic strengths (B) and a function of time under 365 nm light illumination (C).

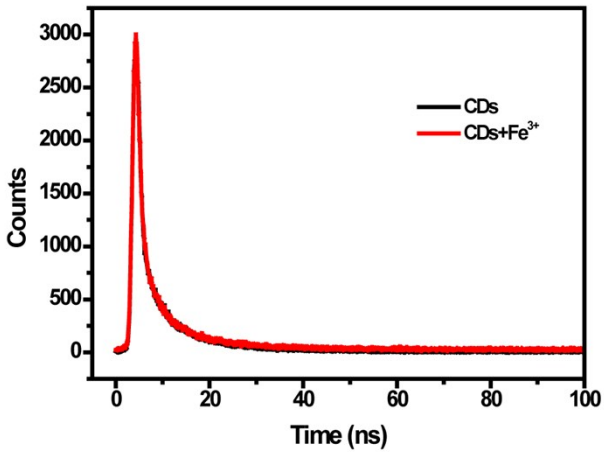

Fig. S4 Fluorescence decay curves of CDs in the absence and presence of Fe(III) upon excitation at 300 nm.

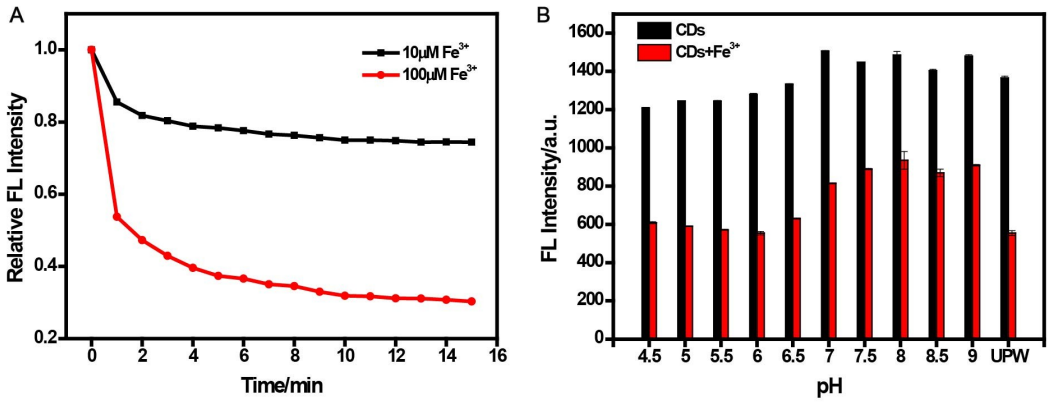

Fig. S5 (A) The variation of relative FL intensity of CDs with 10 μM Fe(III) and 100 μM Fe(III) at different time interval. (B) Fluorescence response of CDs in the absence (black) and presence (red) of 100 μM Fe(III) at different pH values (λ_{ex}=320 nm, λ_{em}=400 nm; UPW: ultrapure water).

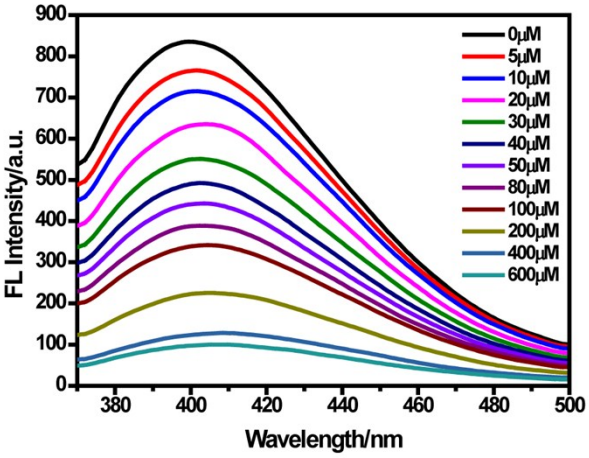

Fig. S6 Fluorescence spectra of CDs in the presence of different concentration of Fe(III) from 0 to 600 μM.

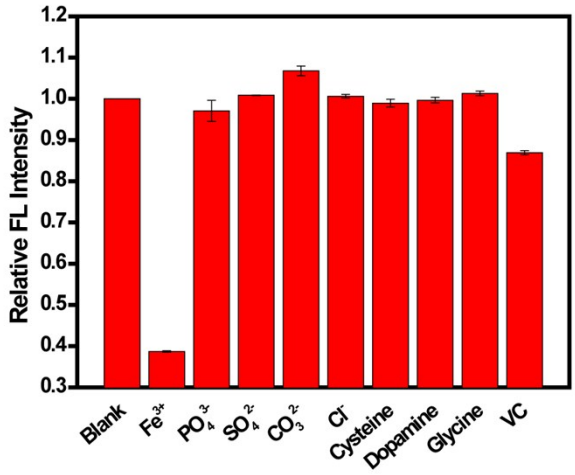

Fig. S7 The selectivity of the sensor toward common anions and organic compounds. The concentration of these anions and organic molecules was 100 μM.

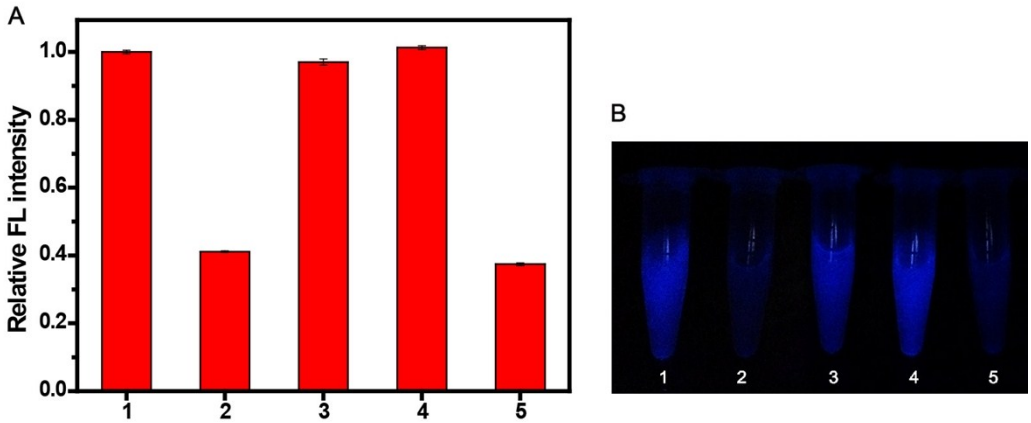

Fig. S8 Fluorescence intensity changes (A) and Photographic images (B) under UV irradiation of CDs (1) and CDs+Fe(III) (2), CDs+Fe(II) (3), CDs+H_2O_2 (4), CDs+Fe(II)+H_2O_2 (5), respectively. (A: [Fe(III)]=[Fe(II)]=[H_2O_2]=100 μM)

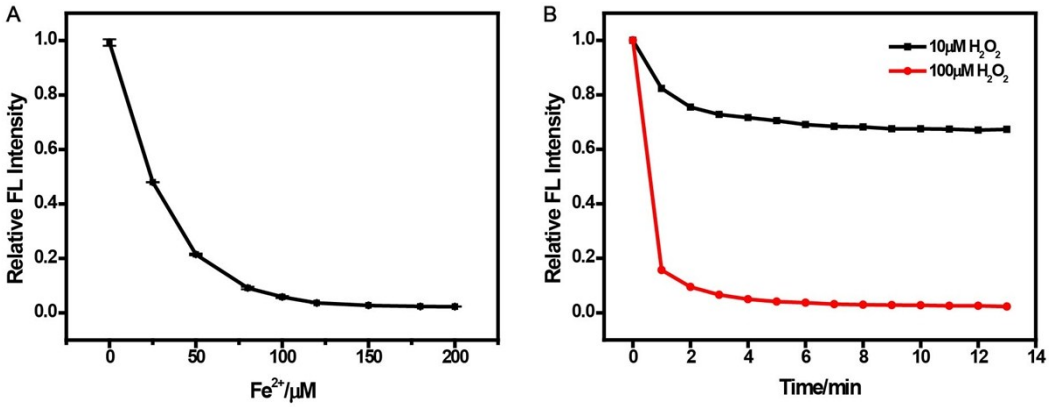

Fig. S9 (A) The variation of relative fluorescence intensities of a solution of CDs and H_2O_2 (100 μM) upon addition different concentration of Fe(II) (0-200 μM). (B) Time-dependent fluorescence intensity of CDs and Fe(II) (120 μM) with the addition of H_2O_2 with different concentrations at room temperature.

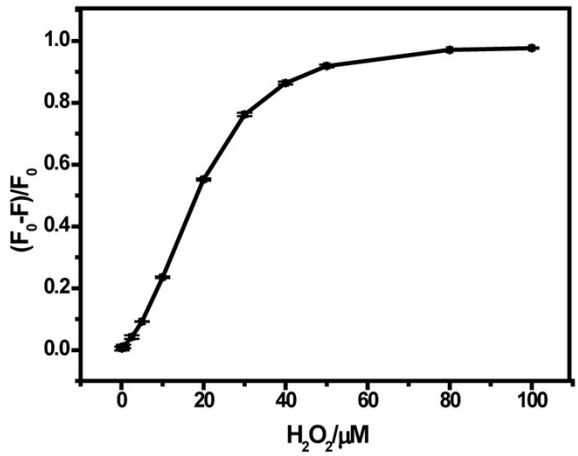

Fig. S10 $(F_0-F)/F_0$ versus concentrations of H_2O_2 from 0 to 100 μM. F_0 and F are the fluorescence intensities of CDs at 400 nm in the absence and presence of H_2O_2, respectively.

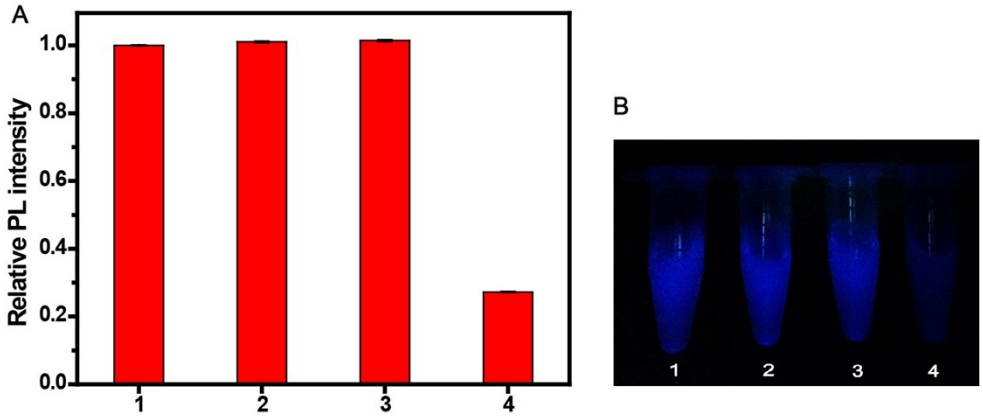

Fig. S11 Fluorescence intensity changes (A) and Photographic images (B) under UV irradiation of CDs (1) and CDs+glucose (2), CDs+GOx (3), CDs+glucose+GOx+Fe(II) (4), respectively. (A: [Fe(II)]=120 μM; [glucose]=50 μM; [GOx]=20 μg/mL)

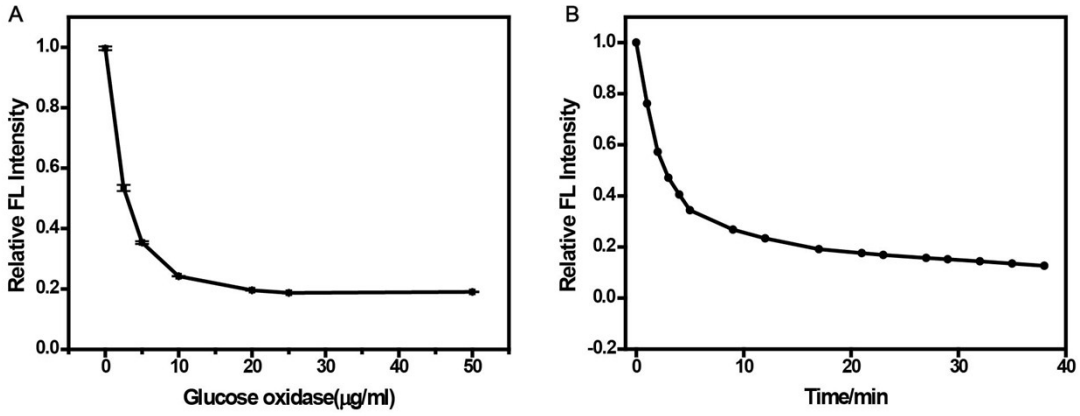

Fig. S12 (A) The variation of the relative fluorescence intensities of a solution of CDs, Fe(II) (120 μM), and glucose (100 μM) upon addition different concentrations of glucose oxidase (0-50 μg/mL). (B) The variation of fluorescence intensities of CDs-based sensor towards glucose at different time intervals (The concentration of glucose is 100 μM).

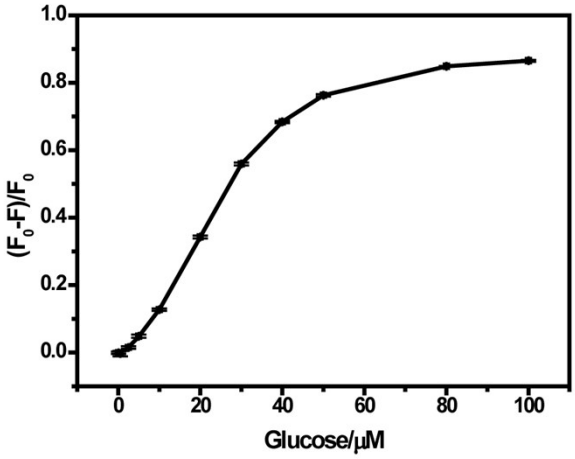

Fig. S13 The relationship between $(F_0-F)/F_0$ and Glucose from 0.1 to 100 μM. F_0 and F are the fluorescence intensities of CDs at 400 nm in the absence and presence of glucose, respectively.

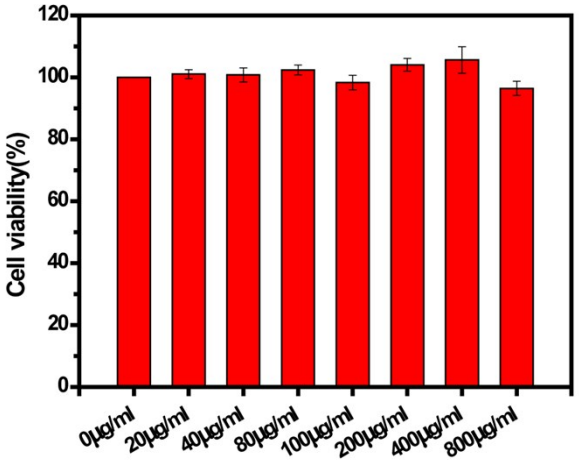

Fig. S14 Viability of HeLa cells in different CDs concentrations.

Table S1. Determination of Fe(III) and glucose in human serum samples.

Analyte	Added (μM)	Found (μM)	Recovery (%, n=3)	RSD (%, n=3)
Fe(III)	5	4.6	92.2	5.3
	20	20.5	102.7	1.8
	40	40.4	101.2	0.6
glucose	5	5.3	107.2	8.2
	20	20.1	100.2	1.0
	40	41.2	103.0	2.1